Total p-p and "p-n" Cross Sections at Cosmotron Energies*

FRANCIS F. CHEN† AND CHRISTOPHER P. LEAVITT, *Brookhaven National Laboratory, Upton, New York,*

AND

ANATOLE M. SHAPIRO,‡ *Brookhaven National Laboratory, Upton, New York, and Harvard University, Cambridge, Massachusetts*

(Received February 29, 1956)

The total proton-proton cross section (excluding Coulomb scattering) has been measured at energies from 410 Mev up to 2.6 Bev, using external beams from the Cosmotron. Fast counting equipment was used to measure the attenuation of the beams through polyethylene, carbon, and liquid H_2 absorbers. At each energy E, $\sigma_{p-p}(E,\Omega)$ was measured as a function of the solid angle Ω subtended by the rear counter at the center of the absorber. The total cross section σ_{p-p} was obtained by a least squares straight line extrapolation to $\Omega=0$. The measured σ_{p-p} as a function of energy rises sharply from 26.5 mb at 410 Mev to 47.8 mb at 830 Mev and then remains approximately constant out to 1.4 Bev, above which energy it decreases gradually to about 42 mb at 2.6 Bev.

Using the same equipment and procedure, we have also measured the D_2O-H_2O difference cross section, called "σ_{p-n}," for protons over the same energy range. From a comparison of "σ_{p-n}," and σ_{p-p}, with the n-p and n-d measurements of Coor *et al.* at 1.4 Bev, it is apparent that one nucleon is "shielded" by the other in the deuteron. This effect is not present at energies below 410 Mev.

Comparing the measured p-p and "p-n" (corrected) cross sections with the results of other high-energy experiments, one may infer the following conclusions: (1) The sharp rise in σ_{p-p} from 400 to 800 Mev results from increasing single pion production, which may proceed through the $T=\frac{3}{2}$, $J=\frac{3}{2}$ excited nucleon state. (2) Above 1 Bev the inelastic (meson production) p-p cross section appears to be approximately saturated at 27–29 mb. (3) The rise in cross section for n-p interaction in the $T=0$ state, associated with the rise in double pion production, implies that double meson production also proceeds through the $T=\frac{3}{2}$ nucleon state. (4) The probable equality of σ_{p-d} and σ_{n-d} at 1.4 Bev implies the validity of charge symmetry at this energy.

I. INTRODUCTION

In the energy region between 95 and 437 Mev, the proton-proton cross section, both differential elastic and total, has been quite thoroughly investigated.[1–7] Discrepancies which existed among various laboratories have recently been resolved[8] and the total elastic cross section is known to remain remarkably constant (between 22 and 24 mb) from 130 to 437 Mev. When proton beams with energies up to 3 Bev became available at the Brookhaven Cosmotron, it was of great interest to determine the behavior of the p-p cross section at these higher energies. In the present experiment the total p-p cross section has been measured in the region from 410 Mev to 2.6 Bev. Experiments[9] are now in progress to determine the cross section for elastic p-p scattering; and the difference between the total and elastic values will give the cross section for inelastic scattering, or meson production, as a function of energy.

The difference in attenuation between D_2O and H_2O absorbers for protons over the same energy range has also been measured. To a first approximation one might expect this difference to correspond to the free neutron-proton cross section, since, at energies above 400 Mev, the proton's wavelength is much smaller than the average internucleon distance in the deuteron. At 408 Mev[2] and 410 Mev[10] the difference cross section, or "σ_{p-n},"[11] has been observed to be approximately equal to the free n-p cross section. It appeared hopeful, therefore, that this method would provide values close to σ_{n-p} at a series of well-defined incident energies. The direct measurement of σ_{n-p} using monoenergetic incident neutrons would be exceedingly difficult at the Cosmotron because the energy spectrum of the emergent neutrons is very broad.[12,13]

Using this broad neutron spectrum, however, σ_{n-p} and σ_{n-d} have been measured by Coor and collaborators.[12] A comparison of the results of their experiment with those of the present one yields information on the charge symmetry of nuclear forces and the properties of the deuteron.

* Research performed under the auspices of the U. S. Atomic Energy Commission.

† Now at Project Matterhorn, P. O. Box 451, Princeton, New Jersey.

‡ Now at the Department of Physics, Harvard University, Cambridge, Massachusetts.

[1] Sutton, Fields, Fox, Kane, Mott, and Stallwood, Phys. Rev. **97**, 783 (1955); **95**, 663 (1954); **90**, 712 (1953).

[2] Marshall, Marshall, and Nedzel, Phys. Rev. **91**, 767 (1953); **92**, 834 (1953); **98**, 1513 (1955).

[3] Chamberlain, Pettengill, Segrè, and Wiegand, Phys. Rev. **93**, 1424 (1954); **83**, 923 (1951).

[4] H. G. de Carvalho, Phys. Rev. **96**, 398 (1954).

[5] C. L. Oxley and R. D. Schamberger, Phys. Rev. **85**, 416 (1952). O. A. Towler, Phys. Rev. **85**, 1024 (1952).

[6] Cassels, Pickavance, and Stafford, Proc. Roy. Soc. (London) **A214**, 262 (1952); J. M. Cassels [private communication to G. Breit (see reference 8)].

[7] Kruse, Teem, and Ramsey, Phys. Rev. **94**, 1795 (1954); **101**, 1079 (1956).

[8] See, for example, G. Breit, *Proceedings of the Fifth Annual Rochester Conference on High-Energy Physics, 1955* (Interscience Publishers, Inc., New York, 1955), p. 145.

[9] Smith, McReynolds, and Snow, Phys. Rev. **97**, 1186 (1955). Also, cloud chamber experiments are in progress, which will be referred to later.

[10] V. A. Nedzel, Phys. Rev. **94**, 174 (1954).

[11] For brevity, we shall hereafter refer to the difference cross section $\sigma_{p-d}-\sigma_{p-p}$ as the "p-n" cross section or "σ_{p-n}," in order to distinguish it from the free neutron-proton cross section $\sigma_{n-p}(=\sigma_{p-n})$.

[12] Coor, Hill, Hornyak, Smith, and Snow, Phys. Rev. **98**, 1369 (1955).

[13] Fowler, Shutt, Thorndike, and Whittemore, Phys. Rev. **95**, 1026 (1954).

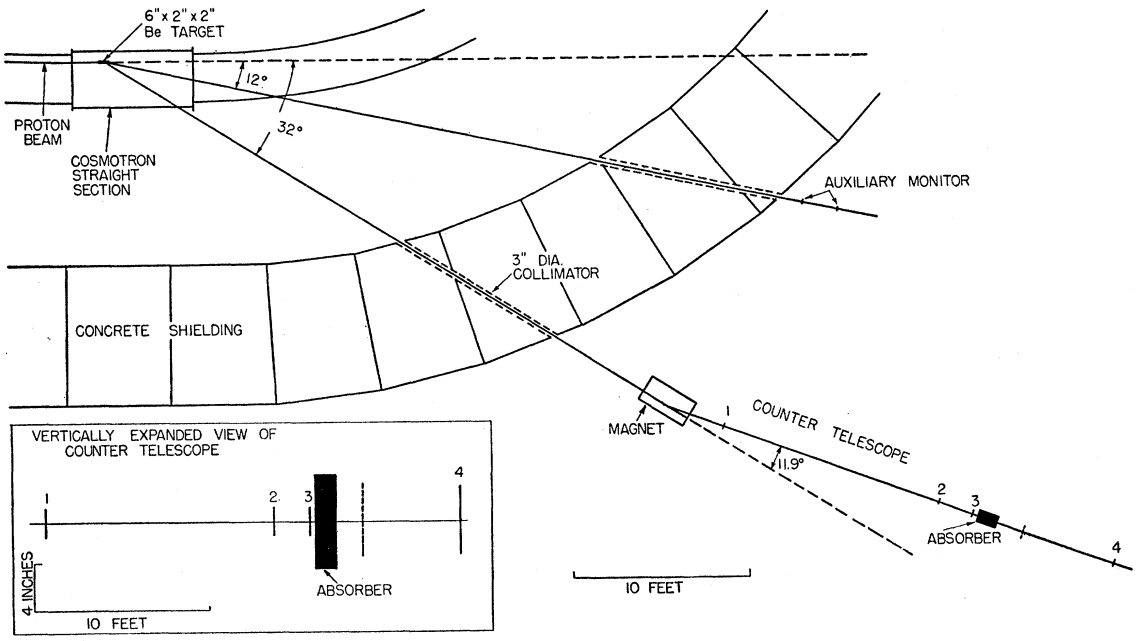

FIG. 1. Experimental arrangement.

Preliminary results of the present work have been reported previously.[14]

II. EXPERIMENTAL METHOD

The total *p-p* cross section at a given energy was obtained in most cases by measuring the attenuation of the proton beam by polyethylene and carbon absorbers. A three-counter telescope monitored the beam incident on the absorbers; and a large fourth counter, in fast coincidence with the first three, measured the transmitted beam.

In order to eliminate the effect of charged secondaries which passed through the fourth counter, the fourth counter was placed at various distances behind the absorbers, and the cross section was determined as a function of the solid angle subtended by this counter at the absorber. These values were extrapolated to zero included solid angle in order to obtain the total cross section.

The minimum angle subtended by the rear counter was chosen so that essentially all protons deflected by single Coulomb scattering did not miss this counter. Hence the extrapolated cross section is the total cross section for all interactions other than Coulomb scattering.

As a check upon the CH_2-C subtraction method, a liquid hydrogen attenuator was also used at two energies.

The D_2O-H_2O attenuation difference was measured under conditions identical to those in the *p-p* measurements. Here also an extrapolation to zero included solid angle was made for determining the total "*p-n*" cross section.

Proton beams of various energies were obtained by two different methods. For energies of 1.5 Bev and below, the experimental arrangement shown in Fig. 1 was used. The internal proton beam of the Cosmotron was made to collapse and strike a 6 in.$\times$2 in.$\times$2 in. beryllium target, located in the east straight section. Particles emerging from the target at an angle of 32° to the forward direction passed out of the straight section through a thin Al window and traveled down a 3-in. diam channel in the 8 ft thick concrete shield surrounding the machine. The smallest angle at which particles from the target could emerge from the Cosmotron without passing through the field of its magnet was 32°. The range of energies in this beam, therefore, had the highest upper limit obtainable in any "direct" beam.

The particles emerging from the collimator then passed through an analyzing magnet, which deflected those of the desired sign and momentum through 11.9° into the counter telescope. The energy of the protons to be studied was varied by changing the current through the analyzing magnet. This experimental arrangement was identical to that used in a previous experiment.[15]

In order to obtain proton beams of sufficient intensity with energies above 1.5 Bev, a second method was used.

[14] Shapiro, Leavitt, and Chen, Phys. Rev. **95**, 663(A) (1954). See also C. P. Leavitt, *Proceedings of the Fifth Annual Rochester Conference on High-Energy Physics, 1955* (Interscience Publishers, Inc., New York, 1955), p. 41; A. M. Shapiro, *Proceedings of the Sixth Annual Rochester Conference on High-Energy Physics, 1956* (to be published).

[15] Chen, Leavitt, and Shapiro, Phys. Rev. **99**, 857 (1955).

It was discovered that, with the internal beam collapsing onto an inside target in the normal manner, a very small fraction of the beam expanded outward radially at the end of the acceleration cycle and flew off tangentially around the machine. By producing at the end of the cycle a fluctuation in the magnetic field of one of the quadrants, this radial "blow-up" beam could be enhanced and concentrated in one direction. Such a beam emerging from the south straight section approximately tangentially was used for the higher energy runs. It passed through a 2-in. diam collimator channel in the shielding wall, and then was analyzed magnetically and counted in the same physical arrangement as was used in the first method.

III. APPARATUS

The equipment used in this experiment has been described in detail in reference 15. Only a brief description will be given here, except for those parts which are new or different.

Counters 1, 2, and 3 were $2\frac{1}{2}$-in. diam plastic scintillators, each viewed edgewise by two matched 1P21 photomultipliers connected in parallel. Counter 4 (No. 4B of reference 15) was a 6-in. diam plastic scintillator, $\frac{1}{2}$ in. thick, viewed edgewise by three matched 1P21's placed symmetrically on its periphery. The pulses from the four counters were amplified, clipped, and placed in fast coincidence in two identical Garwin-type circuits,[16] each having a measured resolving time of 7×10^{-9} sec. In one circuit the first three counters were placed in threefold coincidence, and in the other all four were placed in fourfold coincidence. The output pulses, after amplification, gated discrimination, and stretching to a width of 10^{-7} sec, were counted by 10-megacycle Hewlett-Packard scalers. The efficiency of counter 4 was carefully tested and was found to be very nearly 100% over its entire surface.

The polyethylene and carbon attenuators were chosen to have nearly equal numbers of carbon atoms per cm^2. Two sets of attenuators, each cylindrical in shape and $7\frac{3}{4}$ in. in diameter, but with different lengths, were used. The thinner set was used primarily for the runs with "poorer" geometry, for the purpose of decreasing the spread in the solid angle subtended by counter 4 at the attenuator. The use of two sets also served as a check that the measured cross sections were independent of absorber thickness. The thicker set had surface densities of 32.64 g/cm^2 of CH_2 and 28.18 g/cm^2 of C; the thinner, 14.20 g/cm^2 of CH_2 and 12.20 g/cm^2 of C, corresponding to physical lengths of approximately 14, 7, 6, and 3 inches, respectively. The carbon attenuators were made up of 1-in. thick disks spaced uniformly to fill the volume occupied by the corresponding CH_2 absorber.

For the liquid hydrogen runs, a double-walled Styrofoam container was used, with an inner copper tank having 1-mil windows, through which the proton beam passed. This target presented 2.25 g/cm^2 of liquid H_2 to the beam and 0.4 g/cm^2 of Styrofoam and copper.

Two identical cylinders, 16 in. long and 5 in. in diam with $\frac{1}{16}$-in. brass walls, were used to contain the heavy and light water for the "p-n" measurements. The surface densities were thus 45.1 g/cm^2 of D_2O and 40.6 g/cm^2 of H_2O.

The analyzing magnet had rectangular 36 in.$\times$18 in. pole pieces with a 6-in. gap. The geometry of the experimental arrangement was such that particles from the Cosmotron could not travel directly to the magnet pole faces, nor could any stray particles scattered from the pole faces pass down the counter telescope.

An auxiliary monitor (see Fig. 1), consisting of two counters in coincidence and a separate system of electronics, was placed in another beam. This was needed in the measurement of the beam contamination and provided a continuous check upon the operation of the primary counter telescope.

IV. INVESTIGATION OF THE PROTON BEAM

A. Energy and Energy Resolution

The momentum of the particles passing through the telescope was determined by a calibration of the analyzing magnet. The calibration, by the method of the current-carrying wire,[17] was repeated several times and the results proved to be consistent within 1%.

As a check upon the wire measurement, the range of the particles in copper was also determined for several of the lower energies. Integral range curves taken at 445 and 855 Mev are drawn in Figs. 2 and 3, respectively. The mean range could not be obtained accurately by this method for two main reasons: (1) The attenuation of the particles by nuclear absorption in the copper reduced the number reaching the end of their range to

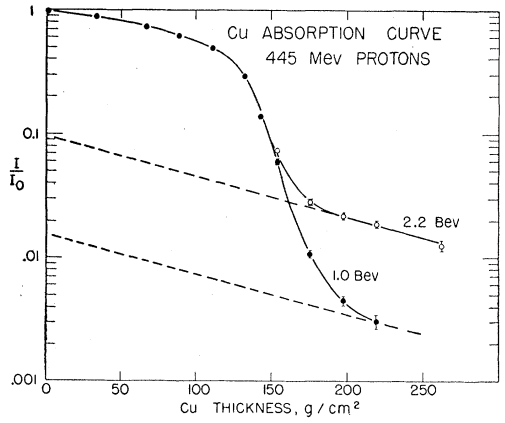

FIG. 2. Integral range curves in copper of the 445-Mev proton beam. The upper curve was obtained with the Cosmotron operating at an energy of 2.2 Bev, and the lower curve at 1 Bev. The extrapolations shown were made using a geometric cross section of $\pi(1.25A^{\frac{1}{3}}\times10^{-13})^2$ cm^2.

[16] R. L. Garwin, Rev. Sci. Instr. **21**, 569 (1950). The circuit was modified along the lines of a distributed amplifier, as suggested by L. Madansky.

[17] DeWire, Ashkin, and Beach, Phys. Rev. **83**, 505 (1951).

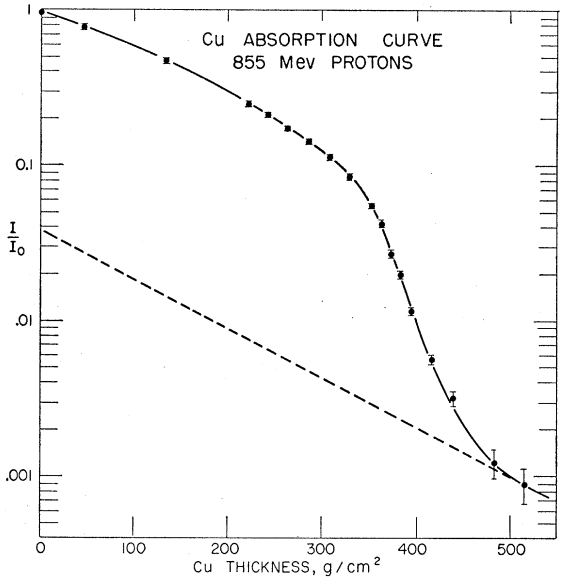

FIG. 3. Integral range curve in copper of the 855-Mev proton beam with the Cosmotron operating at an energy of 2.2 Bev. The extrapolation shown was made using a geometric cross section of $\pi(1.25A^{\frac{1}{3}}\times10^{-13})^2$ cm².

such an extent that good statistics could not be obtained in a reasonable length of time. (2) In order to compute the differential range curve from the integral range measurements, the data had first to be corrected for the nuclear attenuation, and this could not be done with accuracy. However, the range measurements did indicate that the beam particles passing through the telescope consisted predominately of protons having energies consistent with those given by the wire measurements; and they provided information about the energy spread of the beam and the amount of contamination in it.

A stated value of beam energy refers to the mean kinetic energy of the protons emerging from counter 3, except when the statement is made in reference to a cross section measurement, in which case the mean energy at the center of the attenuator is given. These values, as determined by the wire calibration, have an accuracy corresponding to a $\pm2\%$ uncertainty in the value of the beam momentum.

The energy spread of the beam through the telescope corresponds to a momentum spread of 7%, full width at half-maximum, as calculated from the geometry of the experimental arrangement. This width agrees well with that determined from the measured range curves. From the nature of the magnetic analysis, this momentum resolution is of course the same at all energies.

B. Contamination

The analyzed beam passing through the counter telescope contained a small contamination of π^+ mesons, μ^+ mesons, positrons, and possibly K^+ particles, all having the same momentum as the desired protons. The primary contaminant is believed to have been π^+ mesons. In an earlier experiment[18] under very similar experimental conditions it was determined that the ratio of μ^- mesons to π^- mesons in the 32° beam was less than 0.05, and, since the μ-π ratio should be independent of the sign of the charge, μ mesons were a very minor component in the present experiment also. Calculations indicate that the number of high-energy positrons in the beam was negligible. K-particle protion at these energies is completely negligible compared with π-meson production.[19]

The amount of contamination present in the 32° beam was roughly determined by making use of the range measurements in copper. Since at a given momentum the π mesons have a much larger range than the protons, it was possible to obtain an estimate of the number of π mesons or light particles by observing the counting rate for amounts of absorber greater than the proton range. There must be considerable correction for nuclear absorption, and an upper limit for the contamination was set by using the geometric cross section for this correction. The upper limit thus obtained was of the order of a few percent, as indicated by the extrapolations in Fig. 2 and Fig. 3. At the lower momenta the contamination tended to increase, but it was possible to compensate for this by lowering the internal proton beam energy (see Fig. 2).

A better estimate of contamination could be obtained by measuring the counting rate for negative particles of the same momentum as the protons used, and estimating the magnitude of the positive counterpart of these particles from the observed $+/-$ π-meson ratio of Lindenbaum and Yuan[20] in the 32° beam. The measured counting rate for negatives in the present experiment was always less than 0.1% of the positives and the estimated positive contamination less than 0.2%. While Lindenbaum and Yuan's values do not extend above 1.0 Bev/c, the negative counting rates at the higher momenta were so low ($<0.01\%$) that even a ten-fold increase in the $+/-$ ratio would not increase the estimated contamination above 0.2%. Consequently no correction has been introduced for contamination.

The amount of contamination present in the magnetically analyzed "blow-up" beam, although not measured, was also considered negligible. In the "blow-up" beam runs the analyzing magnet deflected into the counter telescope only particles having the maximum momentum available from the machine. Contamination particles of any nature could not be produced with this maximum momentum.

V. EXPERIMENTAL PROCEDURE

The counter telescope position was adjusted in height and angle to maximize the counting rate. It was verified

[18] Shapiro, Leavitt, and Chen, Phys. Rev. **92**, 1073 (1953).
[19] Hill, Salant, and Widgoff, Phys. Rev. **99**, 229 (1955), and private communication.
[20] S. J. Lindenbaum and L. C. L. Yuan (private communication).

that this optimum position coincided with the proton trajectories determined by the current-carrying wire. The 200-ohm cables between the photomultipliers and the coincidence circuits were varied in lengths to test the time resolution of the circuits and to determine the optimum cable lengths. Discriminator bias curves and counter voltage plateau curves were taken for the proper adjustment of the electronics. These were frequently checked.

The beam from the internal Cosmotron target emerged at the end of the acceleration cycle over a period of 30 to 70 milliseconds (msec). The "blow-up" beam for the higher energy measurements was considerably more bunched and appeared over a 5- to 10-msec period. In both cases the coincidence circuit discriminators were biased completely off except for an 80-msec interval centered on the beam pulse. This gating was not needed to eliminate background counts during the "beam-off" time, since there were none, but it did serve to eliminate particles emerging in the 32° beam during the acceleration cycle. These particles had the proper momentum, but since their number and time distribution varied greatly from one Cosmotron pulse to the next, their properties were not investigated.

The threefold counting rate varied from 100 to 1000 per Cosmotron pulse under the various running conditions, with the most frequent rate being between 200 and 400 per pulse. Since the dead time of the entire circuitry was measured to be 2.2×10^{-7} sec, there appeared to be no counting rate loss due to beam bunching, except for some indications of this during the "blow-up" beam runs.

A typical run, for a given proton energy and solid angle subtended by counter 4 at the absorber, consisted of 100 000 threefold pulses, or "triples," with a CH_2 or D_2O attenuator in position and slightly fewer triple counts with the matching C or H_2O attenuator in the beam. The matching absorbers were frequently interchanged during a run in order to eliminate the effects of any slight drifts in the apparatus. Interspersed between these counting periods were frequent 10 000 count runs with no absorber between counters 3 and 4. These provided a continual check upon the operation of the circuits and in the case of the CH_2 and C runs were needed in order to correct for the slightly unequal numbers of C atoms in the two attenuators.

A run, at a given energy and included solid angle, was repeated whenever possible (one or more times) on the same day and also after a period of several weeks or several months. These repeated runs agreed well with each other within statistical expectations.

For the liquid hydrogen runs, two identical containers were used. Before filling, these were interchanged behind counter 3, and their equal attenuation verified. Then one container was filled with liquid hydrogen, and this container and the "dummy" one were frequently interchanged during the run.

The accidental coincidence rate was frequently checked by the insertion of 20 ft of extra cable between one of the counters and the coincidence circuits. This length of extra cable permitted two or more particles resulting from a single revolution of the internal beam of the Cosmotron to pass through the counters and produce an accidental coincidence. With the extra length inserted in channel 4, the accidental rate was generally less than 0.6% of the triples rate. With it in any of the other channels the accidental rate was considerably lower.

Counter 4 was placed at various distances from 20.5 in. to 92.5 in. behind the center of the absorbers. The corresponding half-angle subtended by counter 4 thus ranged from 8.33° down to 1.86°.

VI. CORRECTIONS AND CALCULATIONS

In Sec. IV.B the percentage contamination in the analyzed beam was shown to be very small, and thus no correction has been made for it. Since the contamination consisted primarily of π^+ mesons and since the total π^+-p cross section in this region[21] is not far different from the total p-p cross section, we believe that essentially no error arises from this source.

Although the accidental counting rates due to each individual counter were measured as described in the preceding section, the triple and quadruple accidental rates could not be determined accurately either by measurement or by calculation. They could only be determined if one had a complete knowledge of the time distribution of the pulses in each counter within every Cosmotron pulse. Similarly, it was difficult to determine accurately the effect of "pileup" resulting from the dead time of the electronics.

Because of the difficulty in correcting for the accidental and pile-up rates, these effects were minimized by operating at the low rates of 200 to 400 counts per Cosmotron pulse. With the geometry of the present experimental arrangement it is expected that these effects would tend to decrease the measured value of the cross section. No correction for the pile-up and the accidentals has been made, however. For the measurements in the 32° beam it is estimated that an uncertainty of $(^{+2}_{-1})\%$ from this cause should be included in the final cross sections. In the blow-up beam, which was considerably more bunched than the 32° beam, the measured accidental rates were two to four times higher. The two highest energy measurements, which were made in this beam, are thus subject to considerably more uncertainty (see Secs. VII.A and VII.B).

The contribution of single Coulomb scattering was negligible for the angles and energies employed (see Sec. II).

The only correction that has been applied to the measured transmissions has been for the multiple Coulomb scattering of beam particles out of counter 4

[21] Clark, Cool, Madansky, and Piccioni, *Proceedings of the Fifth Annual Rochester Conference on High-Energy Physics, 1955* (Interscience Publishers, Inc., New York, 1955).

by the CH_2 and C absorbers. Since the CH_2 absorbers had a larger surface density than the C absorbers, a slightly larger percentage of the beam was multiply scattered out of counter 4 by the former than by the latter, and thus the apparent cross section was larger than the true cross section. The fraction of the beam $(1-F)$ multiply scattered out of counter 4 is a function of the beam energy, the surface density of the attenuators, the geometry of the counter telescope, and the transverse distribution of the beam incident upon counter 4 with no intervening attenuators. The dependence of F upon these quantities has been calculated by Sternheimer.[22] The resulting correction can be expressed in the form of a cross section

$$\sigma_m = -(1/Nx)[\ln F_{CH_2} - a \ln F_C], \quad (1)$$

where Nx is the number of hydrogen atoms per cm² in the CH_2 absorber, a is the ratio of the number of carbon atoms per cm² in the CH_2 absorber to the number in the C absorber, and $(1-F_{CH_2})$ and $(1-F_C)$ are the fractions of the beam multiply scattered out of counter 4 by the CH_2 and C attenuators, respectively.

The values of F could not be determined exactly because of uncertainties in several factors in the calculation, primarily the transverse beam distribution. These factors are discussed in detail in reference 15, Sec. VI.B. Because of the uncertainty in the calculation of F, and consequently in σ_m, no runs were considered for which F_{CH_2} (and thus F_C also) was computed to be less than 0.90. In Table I are presented the values of the multiple scattering correction σ_m in millibarns, with the estimated uncertainties, for the remaining runs which satisfied this criterion. These values apply to the thicker CH_2-C absorber set; the correction for the thinner set was negligible for the poorer geometries at which it was used. It is apparent that the correction σ_m is appreciable only at the lower proton energies and the smaller values of Ω, the solid angle subtended by counter 4 at the absorber.

For the liquid hydrogen runs at proton energies of 855 and 1300 Mev the multiple scattering correction was negligible at all solid angles down to the smallest that was measured, 4.53 millisteradians (msterad). In the D_2O and H_2O measurements, the multiple scattering from the two attenuators was equal, and thus no correction was necessary.

TABLE I. Multiple scattering correction σ_m in millibarns.

Proton energy, Mev	Subtended solid angle Ω, millisteradians						
	3.32	7.33	14.6	28.1	43.3	47.8	76.2
410			1.9±0.6	0.4±0.4	0.2±0.2	0.1±0.1	
535		3.1±0.9	0.7±0.5	0.3±0.3	0.1±0.1		
615		1.9±0.6	0.4±0.4	0.2±0.2	0 ±0		0±0
740		1.0±0.5			0 ±0		
830	2.7±0.9	0.7±0.4	0.2±0.2	0 ±0	0 ±0	0 ±0	0±0
1075	1.5±0.5	0.4±0.2	0.1±0.1	0 ±0	0 ±0	0 ±0	0±0
1275	0.7±0.4	0.2±0.2	0 ±0	0 ±0	0 ±0		0±0
1490	0.4±0.2	0.1±0.1	0 ±0	0 ±0	0 ±0		
2000	0.0±0.1	0 ±0	0 ±0	0 ±0	0 ±0		
2600	0 ±0	0 ±0	0 ±0	0 ±0	0 ±0		

[22] R. M. Sternheimer, Rev. Sci. Instr. **25**, 1070 (1954).

For each polyethylene-carbon run at a proton energy E and included solid angle Ω, the p-p cross section is given by the relation

$$\sigma_{p-p}(E,\Omega) = (1/Nx)[\ln R_{CH_2} - a \ln R_C - (1-a)\ln R_0] - \sigma_m, \quad (2a)$$

where R_{CH_2}, R_C, and R_0 are the measured ratios of triple to quadruple coincidences for the CH_2 absorber, the C absorber, and no absorber, respectively. The other symbols have the same meaning as in Eq. (1). For the liquid hydrogen runs the equation becomes

$$\sigma_{p-p}(E,\Omega) = (1/Nx)[\ln R_{\text{filled}} - \ln R_{\text{dummy}}]. \quad (2b)$$

where Nx is the number of hydrogen atoms per cm² in the liquid state, and R_{filled} and R_{dummy} are the measured triple to quadruple ratios for the filled and dummy attenuators, respectively. The "p-n" cross section is determined from the similar equation

$$\text{“}\sigma_{p-n}(E,\Omega)\text{”} = (1/Nx)[\ln R_{D_2O} - \ln R_{H_2O}], \quad (3)$$

where the symbols have the obvious meanings.

The standard deviations in the computed cross sections due to counting statistics were determined in the following manner. For a given run composed of T triple coincidence counts and Q quadruple coincidence counts, the relative standard deviation of the ratio $R=T/Q$ is

$$\epsilon(R)/R = [1/Q - 1/T]^{\frac{1}{2}},$$

since the T and Q counts are statistically related. The statistical standard deviation for $\sigma_{p-p}(E,\Omega)$ derived from Eq. (2a) thus becomes

$$(1/Nx)\left[\left(\frac{1}{Q_{CH_2}} - \frac{1}{T_{CH_2}}\right) + a^2\left(\frac{1}{Q_C} - \frac{1}{T_C}\right) + (1-a)^2\left(\frac{1}{Q_0} - \frac{1}{T_0}\right)\right]^{\frac{1}{2}}. \quad (4)$$

Since a is very close to 1, the last term in the brackets is negligible. The deviations for Eqs. (2b) and (3) follow the same form as Eq. (4).

VII. RESULTS

A. Total p-p Cross Sections

For each run $\sigma_{p-p}(E,\Omega)$ was calculated from the appropriate Eq. (2), but without subtracting σ_m in Eq. (2a). All runs at a given E and Ω, and for a given CH_2-C absorber set, were then combined with proper statistical weighting. From each combined value the appropriate σ_m was subtracted. It was observed that the cross sections measured with the thick and the thin CH_2-C sets agreed well, so these values were combined in the same manner, treating the error in σ_m as though it were a random one. The resulting cross sec-

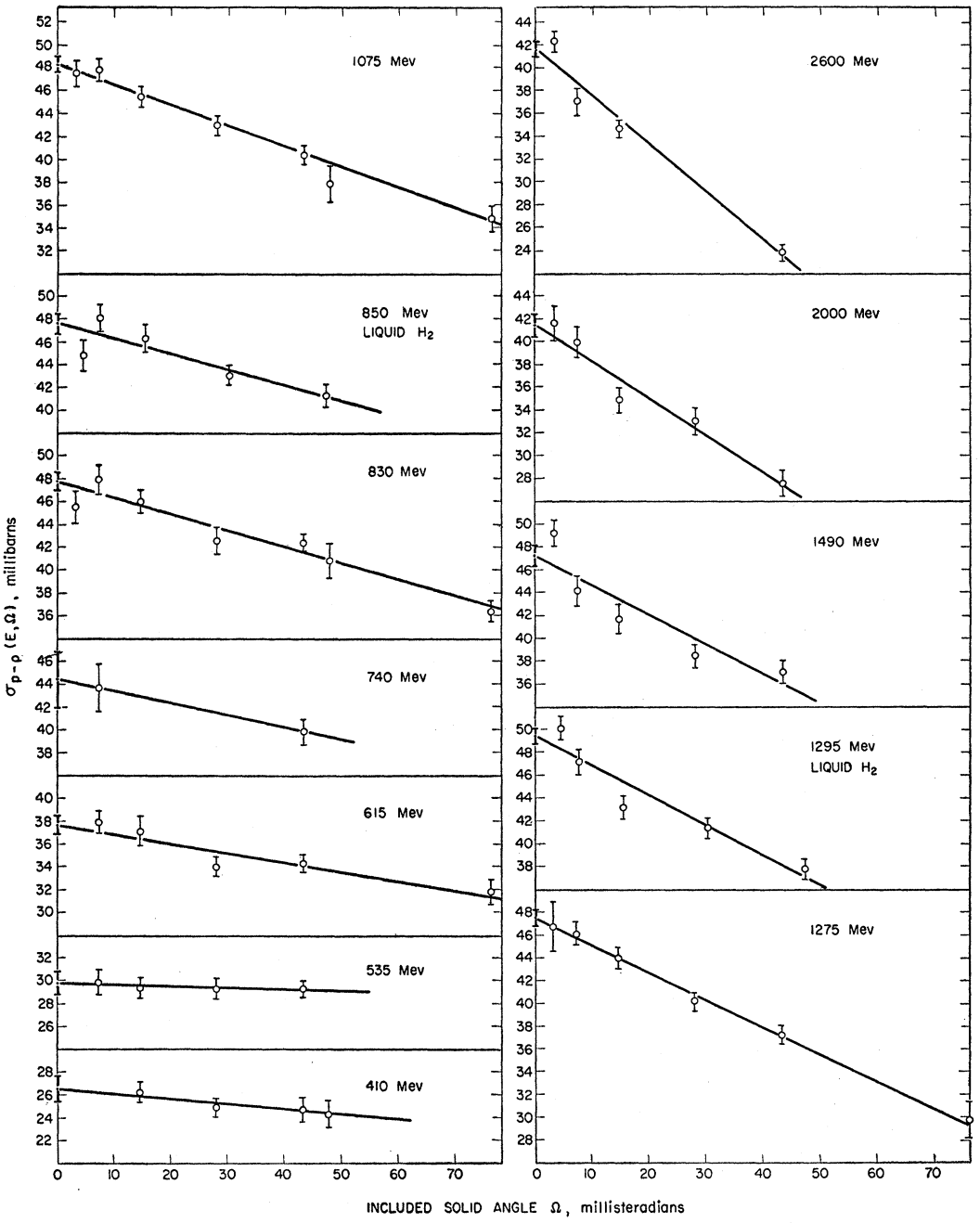

FIG. 4. The measured values of $\sigma_{p-p}(E,\Omega)$, corrected for multiple Coulomb scattering, plotted as a function of the included solid angle Ω for the various proton kinetic energies E that were studied. The straight lines were fitted to the data by least squares calculations.

tions for each E are plotted as a function of Ω in Fig. 4. The standard deviation for each point combines the statistical error and the uncertainty in the multiple scattering correction.

In order to obtain the value of the total nuclear cross section at each energy it is necessary to extrapolate the measured values to zero solid angle. Since the points as plotted in Fig. 4 lie very well along straight lines in most cases, straight lines have been fitted to them by least square calculations which weighted each point inversely as the square of its standard deviation. The calculated lines are drawn in Fig. 4, and the values of the total cross sections thus determined are presented in Table II, column 2. In column 3 the errors as obtained from the least squares calculations are listed. These errors include only the statistical counting error and the uncertainty in the multiple-scattering correction, but of course they depend also on the length of the extrapolation.

An extrapolation in this manner assumes that the differential cross section per unit solid angle for the scattering or production of a charged particle at an

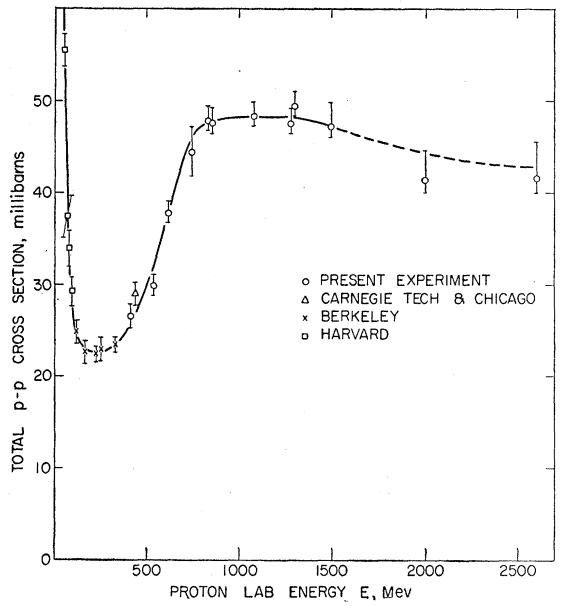

FIG. 5. The total proton-proton cross sections σ_{p-p} as a function of the proton lab energy E. The errors indicated on each point of the present experiment are over-all standard deviations. Only a few of the values obtained in other experiments have been plotted. References: Carnegie Tech—reference 1; Berkeley—reference 3; Harvard—reference 7; Chicago—reference 28.

angle θ, which we shall call $d\Sigma/d\Omega$, is constant from 0° out to the largest angle measured. This assumption is unlikely to be correct. The elastic $d\sigma/d\Omega$ is strongly peaked forward at the higher energies,[9,23–27] and particle production is also.[23] Thus a straight line extrapolation will give an intercept which is lower than the correct cross section. However, unless $d\Sigma/d\Omega$ varies very considerably over the range of angles studied, it can be demonstrated that a nonconstant $d\Sigma/d\Omega$, when integrated from 180° up to $\theta(\Omega)$, will give values of $\sigma(\Omega)$ which can be well fitted by a straight line over a limited range of Ω.

The deviation of the straight-line intercept from the correct total cross section will increase with increasing proton energy. Assuming different possible shapes for $d\sigma/d\Omega$, it can be shown that the least squares intercept will be low by at most 2% to 3% up to 1275 Mev. This error may increase up to 10–15% at 2.6 Bev, and there is some indication at the higher energies that the points are in fact rising more steeply as Ω decreases. We have included in the total error an estimate of the reasonable uncertainty from this source as indicated below.

In column 4 of Table II the over-all errors in the total cross sections are presented. These errors are composed of the following components:

(a) Least squares standard deviations as listed in Table II, column 3.

(b) Uncertainty in extrapolation: $(_{-1}{}^{+2})\%$, 410–1295 Mev; $(_{-1}{}^{+4})\%$, 1490 Mev; $(_{-1}{}^{+6})\%$, 2000 Mev; $(_{-1}{}^{+8})\%$, 2600 Mev.

(c) Error resulting from neglect of accidentals and pile-up: $(_{-1}{}^{+2})\%$, 410–1295 Mev; $(_{-1}{}^{+3})\%$, 1490 Mev; $(_{-2}{}^{+4})\%$, 2000 Mev; $(_{-3}{}^{+5})\%$, 2600 Mev.

(d) Composition of attenuators: $\pm 1\%$ for all points.

In column 5 of Table II the negatives of the slopes of the least squares straight lines are listed. These are approximately the values of the quantity $d\Sigma/d\Omega$ averaged over the angular interval measured. Since this quantity includes the effects of both elastic scattering and charged particle production, one cannot transform it back into the center-of-mass system; and thus no simple interpretation can be made of it. It does, however, provide an upper limit to the value of the differential elastic cross section at approximately 4° in the laboratory system.

The values of the total σ_{p-p} are plotted in Fig. 5, together with the over-all standard deviation for each point. Also plotted are some of the measurements made at lower energies at other laboratories. Some of these were obtained from attenuation experiments and some were determined from measurements of the differential elastic cross sections at various angles. In the latter case, if the total elastic cross section was not calculated by the authors, the value of $d\sigma/d\Omega(90°)$ was multiplied by 2π; and then the value of the total meson production cross section[28] at the given energy was added in. It is apparent from Fig. 5 that the total cross sections determined in this experiment fit quite smoothly onto the values obtained at lower energies.

TABLE II. The total p-p cross sections determined by least squares straight line extrapolations of the data, and the slopes of the lines. The errors are explained in the text.

Proton energy, Mev	Total σ_{p-p}, mb	Least squares standard deviations, mb	Over-all standard deviations, mb	Least squares slope, mb/sterad	Attenuator
410	26.5	±1.2	$_{-1.3}{}^{+1.4}$	43±36	CH_2-C
535	29.8	±1.0	$_{-1.1}{}^{+1.3}$	13±29	CH_2-C
615	37.7	±0.8	$_{-1.0}{}^{+1.4}$	83±19	CH_2-C
740	44.4	±2.5	$_{-2.6}{}^{+2.8}$	104±66	CH_2-C
830	47.8	±0.8	$_{-1.2}{}^{+1.6}$	143±17	CH_2-C
850	47.6	±0.9	$_{-1.2}{}^{+1.7}$	136±31	Liq. H_2
1075	48.3	±0.7	$_{-1.1}{}^{+1.6}$	180±18	CH_2-C
1275	47.5	±0.8	$_{-1.2}{}^{+1.6}$	238±22	CH_2-C
1295	49.4	±0.7	$_{-1.1}{}^{+1.6}$	258±26	Liq. H_2
1490	47.2	±0.9	$_{-1.2}{}^{+2.6}$	257±33	CH_2-C
2000	41.4	±1.0	$_{-1.4}{}^{+3.2}$	322±37	CH_2-C
2600	41.6	±0.7	$_{-1.6}{}^{+4.0}$	419±24	CH_2-C

[23] Fowler, Garrison, and Morris (to be published); Fowler, Shutt, Thorndike, and Whittemore (to be published); Fowler, Shutt, Thorndike, Whittemore, Cocconi, Tongiorgi-Cocconi, Block, and Harth (to be published).

[24] N. P. Bogachev and I. K. Vzorov, Doklady Akad. Nauk S.S.S.R. **99**, 931 (1954).

[25] Mescheryakov, Neganov, Soroko, and Vzorov, Doklady Akad. Nauk S.S.S.R. **99**, 959 (1954).

[26] Selektor, Nikitin, Bogomolov, and Zombkovsky, Doklady Akad. Nauk S.S.S.R. **99**, 967 (1954).

[27] Meshcheryakov, Bogachev, Neganov, and Piskarev, Doklady Akad. Nauk S.S.S.R. **99**, 995 (1954).

[28] A. H. Rosenfeld, Phys. Rev. **96**, 139 (1954); **96**, 130 (1954).

B. Total "p-n" Cross Sections

For each D_2O-H_2O run, "$\sigma_{p-n}(E,\Omega)$" was computed according to Eq. (3). The values at a given E and Ω were combined statistically. The resulting cross sections for each E are plotted as a function of Ω in Fig. 6. The errors indicated are due solely to the counting statistics.

In order to obtain the total "σ_{p-n}" at each energy, the data have again been extrapolated to zero solid angle by least squares straight lines. The uncertainty in the extrapolation resulting from a nonconstancy of $d\Sigma/d\Omega$ is less in the "p-n" case because the slopes of the straight lines are smaller than the corresponding p-p slopes.

However, an additional uncertainty is present in the extrapolation because of the binding of the neutron in the deuteron. We have assumed so far that the neutrons in deuterium are essentially free when struck by the fast protons. This cannot be correct when, in elastic p-n scattering, the recoil neutron is given an energy comparable to its binding energy in the deuteron. This occurs only when the proton is scattered through a very small angle. In order to determine what effect this has on the total "σ_{p-n}," three different least squares straight lines have been fitted to the data at each energy: (1) one using all the measured points, (2) one omitting those measurements made with counter 4 subtending smaller angles than θ_c, where θ_c is the lab angle at which the proton is scattered in an elastic p-n collision with the recoil neutron receiving a lab energy of 2.225 Mev, and (3) one omitting those points made at angles smaller than θ_{2c}, where θ_{2c} is the proton scattering angle corresponding to a recoil neutron energy of 4.45 Mev. The values of Ω corresponding to θ_c and θ_{2c} are indicated beneath each graph in Fig. 6 by a long and a short arrow, respectively. The straight line in each graph is based on calculation (2), using θ_c as the cut-off angle.

In Table III are presented the values of the total "p-n" cross sections determined from the three different extrapolations to zero solid angle. The errors indicated are based solely on the counting statistics, but as before they depend also on the length of the extrapolation. The use of the cut-off angles θ_c and θ_{2c} results in larger errors in the zero intercepts since fewer points remain for making the extrapolation and the remaining ones are further from the σ axis. It is apparent from Table III and Fig. 6 that, with the possible exception of the data at 380 Mev, the three intercepts at each energy agree quite well with each other, and the differences which exist result primarily from the change in the number of points used in each calculation.

At 380 Mev there is perhaps a significant decrease in the measured values of "$\sigma_{p-n}(\Omega)$" for angles below θ_c (see Fig. 6). This may indicate the presence of some

TABLE III. The total "p-n" cross sections determined by three least squares straight line extrapolations of the data—(1) with no lower cut-off angle, (2) with a cutoff at θ_c, and (3) with a cutoff at θ_{2c} (see text).

Proton energy, Mev	Total "σ_{p-n}," mb (1)	(2)	(3)
380	28.4±0.6	31.0±1.2	
590	31.0±0.9	31.5±1.6	27.2±3.3
810	28.6±0.8	28.4±1.0	28.1±1.4
1060	30.1±1.2	27.0±1.8	27.0±1.8
1260	32.1±1.1	32.1±1.1	31.6±1.9
1480	33.6±1.6	33.6±1.6	35.4±2.4
2000	34.3±1.2	34.3±1.2	34.3±1.2
2600	31.4±0.8	31.4±0.8	31.4±0.8

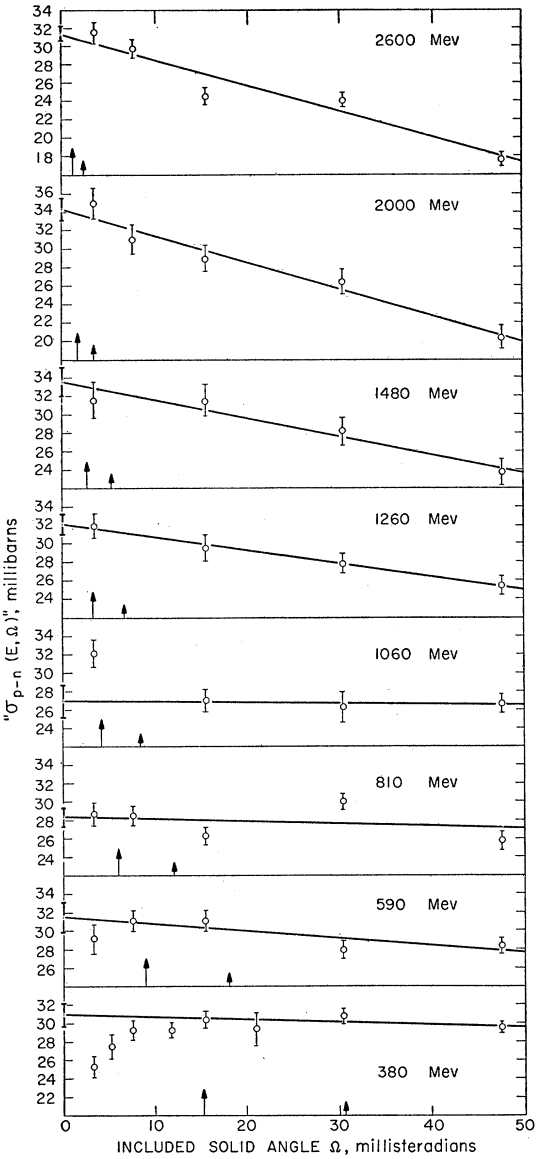

FIG. 6. The measured values of "$\sigma_{p-n}(E,\Omega)$" plotted as a function of the included solid angle Ω for the various proton kinetic energies E that were studied. The long and short arrows indicate the values of Ω corresponding to θ_c and θ_{2c} at each proton energy, as described in the text. The straight lines were fitted to the data by least squares calculations using only those points above the cut-off angle θ_c.

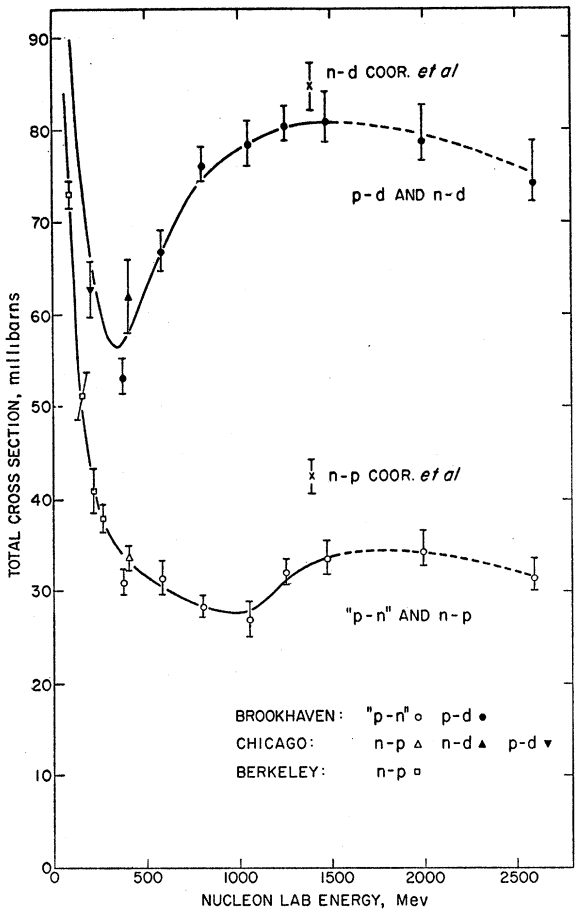

FIG. 7. The total "σ_{p-n}" and σ_{p-d} as a function of the nucleon lab energy E. The errors indicated on each point of the present experiment are over-all standard deviations. References: Brookhaven—present experiment; Coor *et al.*—reference 12; Chicago—reference 10 and 4; Berkeley—references i, j, and q of Table VI.

interference in the deuteron in this angular region, but the data are not sufficiently precise to establish this. Because of this possibility, extrapolation (2) has been taken to represent the best values of the total *p-n* cross section. These values are relisted in Table IV together with the over-all standard deviation in each. They are plotted as a function of the proton lab energy in Fig. 7.

The over-all errors in the total cross section consist of the following components:

(a) Least squares standard deviations as listed in Table IV, column 3.

(b) Uncertainty in extrapolation: $(_{-1}{}^{+2})\%$, 380–1480 Mev; $(_{-1}{}^{+4})\%$, 2000–2600 Mev.

(c) Error resulting from neglect of accidentals and pile-up: $(_{-1}{}^{+2})\%$, 380–1260 Mev; $(_{-1}{}^{+3})\%$, 1480 Mev; $(_{-2}{}^{+4})\%$, 2000 Mev; $(_{-3}{}^{+5})\%$, 2600 Mev.

(d) Composition of attenuators: $\pm 1\%$ for all points.

C. Total *p-d* Cross Sections

Since the "σ_{p-n}" determined in this experiment is strictly $\sigma_{p-d}-\sigma_{p-p}$, the sum of σ_{p-p} and "σ_{p-n}" is exactly σ_{p-d}. To obtain the total *p-d* cross sections most precisely, $\sigma_{p-p}(E,\Omega)$ and "$\sigma_{p-n}(E,\Omega)$" should each be determined for the same values of E and Ω, added together, and then extrapolated to zero solid angle. This could not be done with the present apparatus, but an essentially equivalent result is obtained by the addition of the total *p-p* and "*p-n*" cross sections as determined above.

In this case one does not want to eliminate the effects of the binding of the neutron in the deuteron as was desirable above. Hence the values of "σ_{p-n}" as determined by extrapolation (1) have been used. To these have been added the total *p-p* cross sections interpolated from the smooth curve through the measurements drawn in Fig. 5. The resulting total *p-d* cross sections are listed in Table IV, column 6, and are also drawn in Fig. 7.

VIII. DISCUSSION

A. *p-p* Cross Sections

The variation of the total *p-p* cross section with energy (Fig. 5) exhibits three prominent features. These are the twofold increase in σ_{p-p} between 400 and 800 Mev, its constancy at a value of approximately 48 mb from 800 Mev to 1.4 Bev, and the possible gradual decline in σ_{p-p} above 1.4 Bev.

The sharp rise in the cross section after the long plateau from about 150 to 400 Mev can be attributed to meson production, as is evidenced by the difference between the total and elastic cross sections. The differential elastic cross section above 440 Mev has been measured in several experiments.[9,23–27] In Fig. 8 are plotted the values of the total elastic cross sections determined in these experiments.[29] Also drawn in this figure are the "best" curves through the elastic σ_{p-p} points and through the total σ_{p-p} points of Fig. 5,

TABLE IV. The total "*p-n*" and *p-d* cross sections determined by least squares straight line extrapolations of the data and the slopes of the "σ_{p-n}" lines. The errors and method of calculation are explained in the text.

Proton energy, Mev	Total "σ_{p-n}", mb	Least squares standard deviations, mb	Over-all standard deviations, mb	Least squares slope, mb/sterad	Total σ_{p-d}, mb
380	31.0	±1.2	$_{-1.3}{}^{+1.5}$	29±10	$53.2_{-1.8}{}^{+2.1}$
590	31.5	±1.6	$_{-1.7}{}^{+1.9}$	74±19	$66.8_{-2.0}{}^{+2.4}$
810	28.4	±1.0	$_{-1.1}{}^{+1.3}$	23±34	$76.0_{-1.6}{}^{+2.1}$
1060	27.0	±1.8	$_{-1.9}{}^{+2.0}$	7±49	$78.3_{-2.2}{}^{+2.6}$
1260	32.1	±1.1	$_{-1.2}{}^{+1.5}$	140±12	$80.3_{-1.5}{}^{+2.2}$
1480	33.6	±1.6	$_{-1.7}{}^{+2.0}$	195±24	$80.8_{-2.1}{}^{+3.3}$
2000	34.3	±1.2	$_{-1.5}{}^{+2.3}$	287±39	$78.7_{-2.1}{}^{+3.9}$
2600	31.4	±0.8	$_{-1.3}{}^{+2.2}$	281±25	$74.2_{-2.0}{}^{+4.6}$

[29] In the Brookhaven cloud chamber experiments[23] the ratio of the total elastic cross section to the inelastic cross section at three energies has been determined with greater accuracy than the absolute values of these cross sections. We have thus combined their ratios with our measurements of the total σ_{p-p} to obtain the values of the elastic cross section indicated in Fig. 8 by the open circles. We are grateful to these experimenters for informing us of their results prior to publication.

TABLE V. Total nucleon-nucleon and nucleon-deuteron cross sections at approximately 1.4 Bev. "σ_{p-n}" $\equiv\sigma_{p-d}-\sigma_{p-p}$, and "$\sigma_{n-n}$" $\equiv\sigma_{n-d}-\sigma_{n-p}$.

	Lab energy Mev	σ_{p-p} mb	"σ_{n-n}" mb	"σ_{p-n}" mb	σ_{n-p} mb	σ_{p-d} mb	σ_{n-d} mb
Present experiment	1400	47.7_{-1}^{+2}		33.1_{-1}^{+2}		80.8_{-2}^{+3}	
Coor *et al.*[a]	~1400		42.2±1.8		42.4±1.8		84.6±2.5

[a] See reference 12.

together with a curve which is the difference between the total and elastic curves. The difference curve represents the inelastic or meson production cross section.

It is interesting to note that the center of the rise in the inelastic cross section occurs at approximately 630 Mev. At this energy the total kinetic energy available in the center-of-mass system is 293 Mev, which corresponds to the peak of the π^+-p scattering cross section in the π-p c.m. system.[30] This correspondence suggests that the meson production, which is mainly single π^+ production below 1 Bev,[23] is occurring through an intermediate excited nucleon state

$$p+p\rightarrow n+\underbrace{(\text{excited proton state})}_{\searrow\ \pi^++p}. \qquad (5)$$

The cloud chamber measurements[23] of the angular and energy distributions provide additional evidence for this process.

The shape of the elastic σ_{p-p} curve (Fig. 8) in the region from 300 to 440 Mev was not determined solely by the indicated elastic measurements. The total meson production cross sections are quite well known for energies up to 440 Mev[28]; and these, together with our measurements, help determine the shape of the elastic curve in this energy region. One observes that the elastic σ_{p-p} is rising slightly from 300 to about 500 Mev. There appears thus to be a broad maximum in the elastic cross section in the region of 500–600 Mev. This maximum may be a further indication of the influence of the ($T=\frac{3}{2}$, $J=\frac{3}{2}$) resonance state, and in any case appears to be associated with the sharp rise in the inelastic cross section. A rise in the elastic σ_{p-p} above 400 Mev may be expected, since there should be increasing diffraction scattering accompanying the increasing inelastic cross section.

Assuming the curves as drawn in Fig. 8 are approximately correct, the inelastic cross section remains remarkably constant from 1.0 to 2.6 Bev. In this energy region, double and triple meson production are becoming predominant,[23] and yet the total inelastic cross section remains between 27 and 29 mb. The proton-proton cross section thus appears to level off as though the p-p interaction were saturated in so far as meson production is concerned. This cannot be exactly right, however, since the elastic cross section appears to be significantly less than the inelastic one. For a "black sphere" the two would be equal.

From the value of the inelastic cross section in the high-energy region, approximately 28 mb, one obtains the corresponding p-p interaction radius of about 9.4×10^{-14} cm. This is comparable with the "size" of the proton's charge and magnetic moment distributions as determined by electron-proton scattering experiments.[31]

B. Total "p-n" Cross Sections

The values of "σ_{p-n}" listed in Table IV are presumably not affected by the deuteron binding, since the collisions involving low momentum transfers have been excluded from the extrapolations to zero solid angle. It is clear, however, from a comparison with the neutron experiment of Coor *et al.*[12] that the deuteron difference cross section "σ_{p-n}" is not equal to the free n-p cross

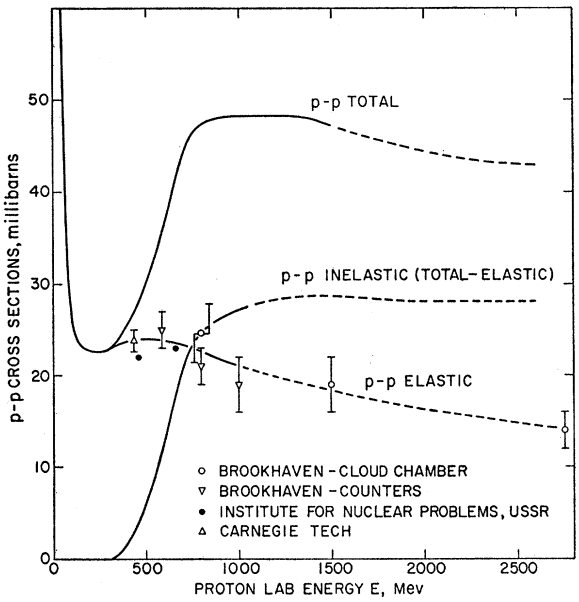

FIG. 8. The total, elastic, and inelastic p-p cross sections as a function of proton energy. The plotted points all represent measurements of the elastic p-p cross section. The inelastic curve (except below 440 Mev) was obtained by subtracting the elastic curve from the total p-p curve. References: Brookhaven cloud chamber—reference 23; Brookhaven counters—reference 9; Institute for Nuclear Problems, U.S.S.R.—references 24 and 27; Carnegie Tech—reference 1.

[30] Ashkin, Blaser, Feiner, Gorman, and Stern, Phys. Rev. **96**, 1104 (1954); S. J. Lindenbaum and L. C. L. Yuan, Phys. Rev. **100**, 306 (1955).

[31] R. Hofstadter and R. W. McAllister, Phys. Rev. **98**, 217 (1955).

section, at least at the higher energies. In other words, it cannot be assumed even at these high energies that the total deuteron cross section is the sum of the individual nucleon-nucleon cross sections.

In the neutron experiment[12] σ_{n-p} was determined to be 42.4±1.8 mb at an average neutron energy of 1.4 Bev. The detector used was primarily sensitive to neutrons with energies between 0.8 and 2.2 Bev; but, since σ_{p-p} and "σ_{p-n}" do not vary too much over this energy region, the measured value of σ_{n-p} should not be greatly affected by the broad neutron spectrum used. The value of "σ_{p-n}" determined in the present experiment is (33.1_{-1}^{+2}) mb at 1.4 Bev, or approximately 9 mb less than σ_{n-p}.

A similar discrepancy exists between the *p-p* cross section at 1.4 Bev $[(47.7_{-1}^{+2})$ mb] and the "*n-n*" cross section of 42.2±1.8 mb measured by Coor *et al.*[12] using the D_2O-H_2O subtraction method. The free *n-n* cross section should be equal to σ_{p-p} (excluding electromagnetic effects, as is done in the present experiment) since nuclear forces are believed to be charge symmetric. Hence the measured values of σ_{n-d} and σ_{p-d} at 1.4 Bev are 5.5 to 9.3 mb less than the sums of the free *n-p* plus *n-n* (assumed equal to *p-p*), and the free *p-p* plus *p-n* cross sections, respectively. A summary of these cross sections is presented in Table V.

A discrepancy of this magnitude has been shown to be reasonable by Glauber.[32] He has calculated that the "shielding" of one nucleon by the other should lower the deuteron cross section by approximately 4.5 to 7.2 mb, in agreement with the observed effect. This calculation is uncertain in three respects. (1) The deuteron

TABLE VI. A summary of total nucleon-nucleon and nucleon-deuteron cross sections from 41 Mev to 2.6 Bev. "σ_{p-n}"$\equiv\sigma_{p-d}-\sigma_{p-p}$, and "$\sigma_{n-n}$"$\equiv\sigma_{n-d}-\sigma_{n-p}$.

Experiment	References	Mean energy Mev	σ_{p-p} mb	"σ_{n-n}" mb	"σ_{p-n}" mb	σ_{n-p} mb	σ_{p-d} mb	σ_{n-d} mb
Present experiment		2600	$41.6_{-1.6}^{+4.0}$		$31.4_{-1.3}^{+2.2}$		$74.2_{-2.0}^{+4.6}$ y	
Present experiment		2000	$41.4_{-1.4}^{+3.2}$		$34.3_{-1.5}^{+2.3}$		$78.7_{-2.1}^{+3.9}$ y	
Present experiment		1490	$47.2_{-1.2}^{+2.6}$					
Present experiment		1480			$33.6_{-1.7}^{+2.0}$		$80.8_{-2.1}^{+3.3}$ y	
Coor *et al.*	a	1400		42.2±1.8		42.4±1.8		84.6(±2.5)
Present experiment		1295	$49.4_{-1.1}^{+1.6}$					
Present experiment		1275	$47.5_{-1.2}^{+1.6}$					
Present experiment		1260			$32.1_{-1.2}^{+1.5}$		$80.3_{-1.5}^{+2.2}$ y	
Present experiment		1075	$48.3_{-1.1}^{+1.6}$					
Present experiment		1060			$27.0_{-1.9}^{+2.0}$		$78.3_{-2.2}^{+2.6}$ y	
Present experiment		850	$47.6_{-1.2}^{+1.7}$					
Present experiment		830	$47.8_{-1.2}^{+1.6}$					
Present experiment		810			$28.4_{-1.1}^{+1.3}$		$76.0_{-1.6}^{+2.1}$ y	
Present experiment		740	$44.4_{-2.6}^{+2.8}$					
Present experiment		615	$37.7_{-1.0}^{+1.4}$					
Present experiment		590			$31.5_{-1.7}^{+1.9}$		$66.8_{-2.0}^{+2.4}$ y	
Present experiment		535	$29.8_{-1.1}^{+1.3}$					
Sutton *et al.*	b	437	23.8 ±1.2 + 3.2 ±1[u] =27.0 ±1.5					
Marshall *et al.*	c	429	21.5 ±0.8[v] + 2.8 ±1[u] =24.3 ±1.3					
Marshall *et al.*	c	419	21.5 ±0.8[v] + 2.4 ±0.8[u] =23.9 ±1.1					
Present experiment		410	$26.5_{-1.3}^{+1.4}$					
Nedzel	d	410		28±4		33.7±1.3		62±4
Marshall *et al.*	c	408	24.0 ±1		31.6±2		55.6±2.2	
Present experiment		380			$31.0_{-1.3}^{+1.5}$		$53.2_{-1.8}^{+2.1}$	
Dzhelepov *et al.*	e	380		20.0±1.4		40±4		60±3
Chamberlain *et al.*	f	345	23.9 ±1.2[v] + 0.4 ±0.1[u] =24.3 ±1.2					
Chamberlain *et al.*	f	330	23.4 ±0.9[w] + 0.15±0.05[u] =23.6 ±0.9					
de Carvalho	g	315	24.3 ±1		32.5±4		56.8±5	
Dzhelepov *et al.*	e	300		22				
Fox *et al.*	h	280		16(±4)		33±3		49±5
Marshall *et al.*	c	271	23.1 ±2.1[v]					
DeJuren	i	270		19(±3)		38±1.5		57±3
Chamberlain *et al.*	f	250	22.9 ±1.3[v]					
Chamberlain *et al.*	f	225	22.4 ±0.9[w]					
DeJuren and Moyer	j	220				41±2.4		
de Carvalho	g	208	25.8 ±2.0		37.0±2.0		62.8±3.0	
Alphonce *et al.*	k	169		23.1±2.0		49.2±1.6		72.3±3

[32] R. J. Glauber, Phys. Rev. **100**, 242 (1955), and private communication.

TABLE VI.—*Continued.*

Experiment	References	Mean energy Mev	σ_{p-p} mb	"σ_{n-n}" mb	"σ_{p-n}" mb	σ_{n-p} mb	σ_{p-d} mb	σ_{n-d} mb
Chamberlain *et al.*	f	164	22.6 ±1.3[v]					
DeJuren and Moyer	j	160				51.2±2.6		
Alphonce *et al.*	k	149		24.8±2.0				
Cassels	l	147	25.4 ±1.3[v]					
Marshall *et al.*	c	144	20.2 ±0.7[v]					
Taylor and Wood	m	134	23.7 ±0.9					
Alphonce *et al.*	k	132		25.3±2.4				
Chamberlain *et al.*	f	120	24.8 ±1.3[v]					
Alphonce *et al.*	k	117		27.2±2.4				
Alphonce *et al.*	k	109		29.1±3.6				
Culler and Waniek	n	98.6		32(±4)		76±3		108±5
Kruse *et al.*	o	95	29.2 ±1.6[v]					
		95			65±7[x]			
Bloom and Chamberlain	p	95					94_{-5}^{+7}	
DeJuren and Knable	q	95		31(±4)		73±1.5		104±4
Culler and Waniek	n	94.8		33(±5)		77±5		110±7
Hillman *et al.*	r	88				85.3±2		
Cook *et al.*	s	85		34±3		83±4		117±5
Kruse *et al.*	o	78.5	33.9 ±2.0[v]					
Kruse *et al.*	o	69.5	37.4 ±2.3[v]					
Kruse *et al.*	o	51.8	55.5 ±1.8[v]					
Hillman *et al.*	r	47.5				196±10		
Hildebrand and Leith	t	42		86(±13)		203±7		289±13
Kruse *et al.*	o	41	71.6 ±5.0[v]					

[a] See reference 12.
[b] See reference 1.
[c] See reference 2.
[d] See reference 10.
[e] V. P. Dzhelepov and Yu. M. Kazarinov, Doklady Akad. Nauk S.S.S.R. **99**, 939 (1954); Dzhelepov, Golovin, and Satarov, Doklady Akad. Nauk S.S.S.R. **99**, 943 (1954).
[f] See reference 3.
[g] See reference 4.
[h] Fox, Leith, Wouters, and MacKenzie, Phys. Rev. **80**, 23 (1950).
[i] J. DeJuren, Phys. Rev. **80**, 27 (1950).
[j] J. DeJuren and B. J. Moyer, Phys. Rev. **81**, 919 (1951).
[k] Alphonce, Johansson, Taylor, and Tibell, Phil. Mag. **46**, 295 (1955); A. E. Taylor, Phys. Rev. **92**, 1071 (1953).
[l] See reference 6.
[m] A. E. Taylor and E. Wood, Phil. Mag. **44**, 95 (1953).
[n] V. Culler and R. W. Waniek, Phys. Rev. **95**, 585 (1954); **99**, 740 (1955).
[o] See reference 7.
[p] A. L. Bloom and O. Chamberlain, Phys. Rev. **94**, 659 (1954).
[q] J. DeJuren and N. Knable, Phys. Rev. **77**, 606 (1950).
[r] Hillman, Stahl, and Ramsey, Phys. Rev. **96**, 115 (1954).
[s] Cook, McMillan, Peterson, and Sewell, Phys. Rev. **75**, 7 (1949).
[t] R. H. Hildebrand and C. E. Leith, Phys. Rev. **80**, 842 (1950).
[u] The total meson production cross section was obtained from an analysis of all available production data.
[v] The total elastic p-p cross section was obtained by multiplying the average measured differential elastic cross section by 2π.
[w] Published value was a differential cross section derived from an attenuation measurement assuming isotropy. The number presented here was obtained by multiplying the published value by 2π.
[x] Was obtained from the difference between the two neighboring measurements.
[y] σ_{p-d} is obtained by adding to "σ_{p-n}" the value of σ_{p-p} obtained from a smooth curve through the σ_{p-p} data.

wave function at small distances is not accurately known. The use of different wave functions produces the above-stated variation in the calculated effect. (2) In the absence of experimental evidence spin dependence effects were neglected in the calculation, although it could easily be generalized to include them. These effects might not be negligible even at these energies.[33] (3) Although the shielding calculation was developed for a general form of interaction, in order to obtain numerical results it was necessary to assume a "black sphere" model for the nucleons. It is now clear (see Fig. 8 and Sec. VIII.A) that the "black sphere" model is not entirely adequate. Despite these uncertainties, however, it appears that the shielding calculation of Glauber provides a reasonable explanation for the observed discrepancies at 1.4 Bev.

It should be noted, on the other hand, that in the energy region from ~95 to ~410 Mev the discrepancy between σ_{n-p} and "σ_{p-n}," and between σ_{p-p} and "σ_{n-n}," is very small, if not zero. This can be seen in Table VI, which contains a summary of nearly all the total nucleon-nucleon and nucleon-deuteron cross sections measured from 2.6 Bev down to 41 Mev. In the low-energy region below 410 Mev, the interactions are mainly elastic, and the incident particle wavelengths are much longer. Hence one might expect interference effects in the deuteron to be important and to manifest themselves. It appears, however, that their net effect is essentially negligible, so that in the entire low-energy region the D_2O-H_2O difference cross sections are nearly equal to free neutron cross sections.

A reasonable explanation of the significant difference in the observed deuteron defect at high and low energies may arise from the variation of the nucleon's characteristics with energy. At high energy (above 800 Mev) the nucleon is nearly opaque and may possibly be represented by a purely imaginary potential well

[33] S. Drell (private communication).

TABLE VII. Values used to obtain the corrected n-p cross section "$\sigma_{p-n}{}^{\text{corr}}$" and the total $T=0$ state cross section $\sigma_{T=0}$.

Proton energy Mev	σ_{p-p} mb	"σ_{p-n}" mb	$\frac{1}{1-C\sigma_{p-p}}$	"$\sigma_{p-n}{}^{\text{corr}}$" mb	$\sigma_{T=0}$ mb
400	25.4	33.6	1.00	33.6	41.8
500	29.9	31.8	1.020	32.4	34.9
600	36.5	30.5	1.050	32.0	27.4
700	43.9	29.4	1.096	32.2	20.6
800	47.3	28.6	1.139	32.5	17.3
900	48.0	27.9	1.177	32.8	17.6
1000	48.2	27.7	1.215	33.6	19.0
1100	48.2	28.4	1.215	34.4	20.6
1200	48.2	30.1	1.215	36.6	25.0
1300	48.1	31.9	1.214	38.8	29.5
1400	47.7	33.1	1.211	40.1	32.5
1500	47.1	33.8	1.209	40.8	34.5
1600	46.4	34.2	1.203	41.1	35.8
1700	45.8	34.4	1.200	41.3	36.8
1800	45.3	34.5	1.200	41.4	37.5
1900	44.8	34.4	1.196	41.1	37.4
2000	44.3	34.3	1.192	40.9	37.5
2100	43.9	34.0	1.191	40.5	37.1
2200	43.5	33.6	1.190	40.0	36.5
2300	43.3	33.2	1.189	39.4	35.5
2400	43.1	32.7	1.188	38.8	34.5
2500	42.9	32.2	1.187	38.2	33.5
2600	42.8	31.6	1.187	37.4	32.0

(see also reference 23). At low energies (below 400 Mev) there is essentially no inelastic interaction, and the nucleon may be represented by a purely real potential well.

Since monoenergetic sources of neutrons at high energies are not available and since it would be very difficult to measure the variation of σ_{n-p} with incident neutron energy by means of present-day machines and techniques, it is of considerable interest to convert our measured values of "σ_{p-n}" into free n-p cross sections. Above 1 Bev the general shielding calculation[32] should give reasonably accurate corrections. These corrected cross sections will be called "$\sigma_{p-n}{}^{\text{corr}}$." The method used in obtaining the "$\sigma_{p-n}{}^{\text{corr}}$" values is described in Appendix I.

These calculated values are listed in Table VII, column 5. In Fig. 9 a smooth "$\sigma_{p-n}{}^{\text{corr}}$" curve is drawn, together with smooth curves fitted to the σ_{p-p} and "σ_{p-n}" data (see Figs. 5 and 7).

It is apparent that "$\sigma_{p-n}{}^{\text{corr}}$" varies much differently with energy than does σ_{p-p}. The sharp rise in σ_{p-p} from 400 to 800 Mev is completely absent, and "$\sigma_{p-n}{}^{\text{corr}}$" in this region is instead almost constant. There is a small rise in "$\sigma_{p-n}{}^{\text{corr}}$" above 1 Bev, in the energy region where σ_{p-p} is very nearly constant. Such differences as these are not unexpected, since the p-p interaction can occur only in an isotopic spin $T=1$ state while the p-n interaction occurs half in the $T=1$ state and half in the $T=0$ state. Thus we can write that

$$\sigma_{p-p}\equiv\sigma_{T=1},$$

and

$$\sigma_{p-n}\equiv\tfrac{1}{2}\sigma_{T=0}+\tfrac{1}{2}\sigma_{T=1},$$

where $\sigma_{T=0}$ and $\sigma_{T=1}$ are the total cross sections for nuclear interaction in the $T=0$ and $T=1$ states, respectively. Assuming that the cross sections "$\sigma_{p-n}{}^{\text{corr}}$," as calculated in Appendix I, are approximately equal to the free p-n cross sections, the values of $\sigma_{T=0}$ can be obtained from the simple equation

$$\sigma_{T=0}=2[\sigma_{p-n}-\tfrac{1}{2}\sigma_{p-p}].$$

These are listed in column 6 of Table VII and are also plotted in Fig. 9.

The shape of the $\sigma_{T=0}$ curve is quite similar to that of $\sigma_{T=1}$ but is displaced to higher energies by about 700 Mev. The curves indicate perhaps that single pion production, which predominates below 1 Bev, proceeds mainly through the $T=1$ state and very little, if at all, through the $T=0$ state. $\sigma_{T=0}$ then rises quite sharply above 1 Bev, where double pion production becomes important.[13,23] These features are to be expected if pion production occurs predominantly in a $T=\frac{3}{2}$ pion-nucleon interaction. Such a $T=\frac{3}{2}$ interaction, involving only one nucleon, cannot occur in a $T=0$ neutron-proton state. Thus meson production would be inhibited in the $T=0$ n-p state at energies below the onset of double meson production. Double pion production *can* occur, however, in the $T=0$ state (as well as in the $T=1$ state) with both mesons being emitted from $T=\frac{3}{2}$ excited nucleon states. Hence, from the coincidence of the sharp rise of single π production with the sharp rise of $\sigma_{T=1}$, and from the coincidence of the rise of double π production with the rise of $\sigma_{T=0}$, one might conclude that pion production proceeds predominately through $T=\frac{3}{2}$ nucleon states.

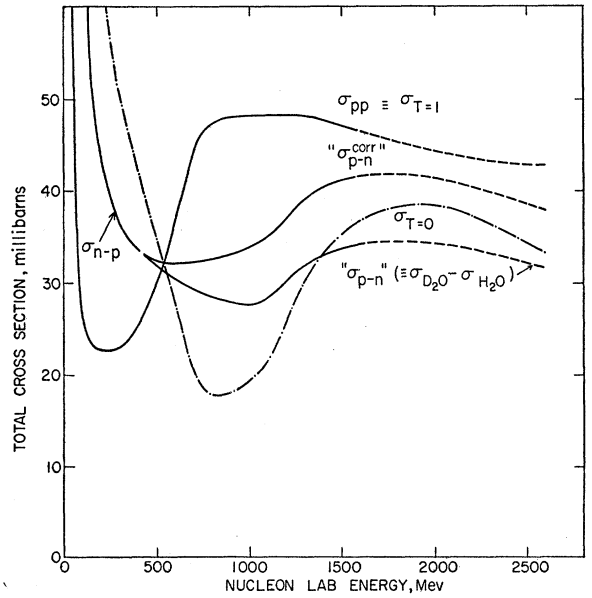

FIG. 9. Derived cross section curves. The σ_{p-p} and "σ_{p-n}" curves are smooth curves drawn through the data (see Figs. 5 and 7). The "$\sigma_{p-n}{}^{\text{corr}}$" curve was obtained from "σ_{p-n}" as described in Appendix I. The derivation of $\sigma_{T=0}$ is described in the text.

C. Total p-d Cross Sections

As can be seen in Table VI, σ_{p-d} and σ_{n-d} are essentially equal at all energies up to 437 Mev. The equality of σ_{p-d} and σ_{n-d} implies the equality of σ_{p-p} and σ_{n-n}, which is required for the charge symmetry of nuclear forces. A comparison of our p-d cross section of (80.8_{-2}^{+3}) mb at 1.4 Bev with the corresponding measurement by Coor *et al.*[12] of $\sigma_{n-d}=84.6\pm2.5$ mb indicates that charge symmetry is still valid at this high energy.

IX. ACKNOWLEDGMENTS

We are indebted to many persons for stimulating and enlightening discussions, among whom we should particularly like to thank Dr. K. Brueckner, Dr. S. Drell, Dr. R. Glauber, and Dr. R. Serber. The assistance of Dr. G. B. Collins, Dr. W. Moore, Dr. L. Smith, Dr. C. Swartz, and the entire Cosmotron Department Staff in the preparation of the experiment and the reliable operation of the Cosmotron is gratefully acknowledged.

APPENDIX I. SHIELDING CORRECTION TO THE MEASURED "σ_{p-n}" VALUES

As discussed in Sec. VIII.B, it is necessary to correct the measured "p-n" cross sections for the shielding of one nucleon by the other in the deuteron. If it is assumed that the nucleon interactions are purely absorptive, as is indicated by the cloud-chamber measurements,[23] Glauber[32] has shown that the total p-d cross section is given by the equation

$$\sigma_{p-d}=\sigma_{p-p}+\sigma_{p-n}-\frac{1}{4\pi}\langle\text{“}r^{-2}\text{”}\rangle_d\sigma_{p-p}\sigma_{p-n}, \tag{6}$$

where σ_{p-n} is the total cross section for nuclear interaction of a proton with a free neutron. The constant $\langle\text{“}r^{-2}\text{”}\rangle_d$ is the expectation value in the deuteron of a function which behaves asymptotically for large neutron-proton separation as r^{-2}; but this function remains finite for small r, where it has a form which depends on the opacity distribution of the individual nucleon.

Since "σ_{p-n}"$\equiv\sigma_{p-d}-\sigma_{p-p}$, we have

$$\sigma_{p-n}=\text{“}\sigma_{p-n}\text{”}+\frac{1}{4\pi}\langle\text{“}r^{-2}\text{”}\rangle_d\sigma_{p-p}\sigma_{p-n}. \tag{7}$$

Also,

$$\sigma_{n-n}=\text{“}\sigma_{n-n}\text{”}+\frac{1}{4\pi}\langle\text{“}r^{-2}\text{”}\rangle_d\sigma_{n-p}\sigma_{n-n}.$$

Since the deuteron wave function at small distances and the opacity distribution of the nucleon are not well determined, we shall evaluate the quantity $\langle\text{“}r^{-2}\text{”}\rangle_d$ from the measured cross sections at 1.4 Bev. Since $\sigma_{p-n}=\sigma_{n-p}$, and assuming that $\sigma_{n-n}=\sigma_{p-p}$, as is indicated by Sec. VIII.C, the deuteron defect for incident protons is $\sigma_{p-n}-\text{“}\sigma_{p-n}\text{”}=\sigma_{n-p}-\text{“}\sigma_{p-n}\text{”}=42.4-33.1=9.3$ mb at 1.4 Bev (see Table V). The deuteron defect for incident neutrons is $\sigma_{n-n}-\text{“}\sigma_{n-n}\text{”}=\sigma_{p-p}-\text{“}\sigma_{n-n}\text{”}=47.7-42.2=5.5$ mb. These two values are equal within the experimental errors, as they should be; and we shall thus use the value of 7.4 mb as the average deuteron defect. (This can be compared with the defects of 4.5, 5.7, and 7.2 mb calculated by Glauber using different deuteron wave functions.)

Substituting the average defect into Eq. (7), we obtain

$$7.4\text{ mb}=\frac{1}{4\pi}\langle\text{“}r^{-2}\text{”}\rangle_d\times47.7\text{ mb}\times42.4\text{ mb}.$$

Hence, $(1/4\pi)\langle\text{“}r^{-2}\text{”}\rangle_d=3.66\times10^{-3}$ mb^{-1}, which will be called the constant C. The equation for σ_{p-n} becomes therefore, from Eq. (7),

$$\sigma_{p-n}=\left[\frac{1}{1-C\sigma_{p-p}}\right]\text{“}\sigma_{p-n}\text{.”} \tag{8}$$

Equation (8) should be quite accurate for energies above 1 Bev, since from 1 Bev to 2.6 Bev the inelastic p-p cross section is practically constant and the proton is nearly "all black" (see Fig. 8). At 400 Mev the deuteron defect is about zero. Between 400 Mev and 1 Bev it is not clear how the deuteron defect varies. In the absence of better information, we shall assume that the correction factor $[1/(1-C\sigma_{p-p})]$ varies linearly from 1.215 at 1 Bev down to 1.000 at 400 Mev (instead of the value of 1.10 which the correction factor would have at 400 Mev if Eq. (8) were still applicable at this energy).

Since this correction is somewhat uncertain, we shall call the corrected cross sections "$\sigma_{p-n}{}^{\text{corr}}$" in order to distinguish them from the true free cross sections σ_{p-n} or σ_{n-p}. The values of the correction factor are listed in column 4 of Table VII. In columns 2 and 3 are the values of σ_{p-p} and "σ_{p-n}," respectively, obtained from smooth curves through the data (see Figs. 5 and 7), which were used in calculating the correction factor and "$\sigma_{p-n}{}^{\text{corr}}$." The cross sections "$\sigma_{p-n}{}^{\text{corr}}$" are listed in column 5 of Table VII and are plotted in Fig. 9.